Article

A new species within the *Enteromius kerstenii* complex (Actinopterygii, Cyprinidae, Smiliogastrinae) from south-western Ethiopia

GERNOT K. ENGLMAIER[1,2,*], MIN CHAI[2], ALEMAYEHU WUBIE[3], RUPERT A. COLLINS[4] & ABEBE GETAHUN[5]

[1]*Institute of Vertebrate Biology, Czech Academy of Sciences, Květná 8, 60365 Brno, Czech Republic*
✉ *gernotenglmaier@gmx.at;* ● *https://orcid.org/0000-0002-9746-4500*
[2]*Natural History Museum Vienna, Burgring 7, A-1010 Vienna, Austria*
✉ *min.chai@nhm-wien.ac.at;* ● *https://orcid.org/0009-0003-6213-2973*
[3]*EIAR-National Fisheries and Aquatic Life Research Center, P.O. Box 64, Sebeta, Ethiopia*
✉ *alemayehuwubie@gmail.com*
[4]*Department of Life Sciences, Natural History Museum, Cromwell Road, London, SW7 5BD, United Kingdom*
✉ *rupert.collins@nhm.ac.uk;* ● *https://orcid.org/0000-0002-9135-1169*
[5]*Department of Zoological Sciences, Addis Ababa University, PO Box 1176, Addis Ababa, Ethiopia*
✉ *abebe12002@yahoo.com;* ● *https://orcid.org/0000-0003-4489-3907*
*Corresponding author

Abstract

A new species of small-sized smiliogastrin barb, *Enteromius gamo* **sp. nov.**, is described from tributaries to lakes Abaya and Chamo in south-western Ethiopia. The new species belongs to a readily diagnosable group commonly identified as *E. kerstenii*, exhibiting a thickened and serrated last unbranched ray in the dorsal fin, a low number of scales in the lateral series (≤ 27), and a yellow, orange or reddish blotch on operculum. Pairwise genetic distances between the new species from Ethiopia and specimens of *E. kerstenii* from close to the type locality in north-eastern Tanzania were 7.5–8.3 % (COI) and 8.9–10.1 % (cytb). *Enteromius gamo* **sp. nov.** is morphologically distinguished from *E. kerstenii* and all examined congeners from Tanzania, Kenya, and Uganda primarily by short anterior (15.8–35.1 %, mean 27.4 %, of snout length) and posterior (63.2–95.7 %, mean 81.0 %, of snout length) barbels. The new species is known only from wetlands and side channels of rivers (Hare, Sile, and Sago) along the western shores of lakes Abaya and Chamo.

Key words: Africa, conservation, endemism, freshwater fish, taxonomy, wetlands

Introduction

High levels of genetic divergence coupled with superficial phenotypic similarity in widely distributed species complexes render taxonomy and species delimitation within the smiliogastrin barb genus *Enteromius* Cope, 1867 difficult, and many problems remain unresolved. Recent integrative taxonomic studies (e.g., Van Ginneken *et al.* 2017; Mamonekene *et al.* 2018; Schmidt *et al.* 2018; Englmaier *et al.* 2020; Maetens *et al.* 2020; Kambikambi *et al.* 2021; Prokofiev *et al.* 2021; Kisekelwa *et al.* 2022), however, have renewed interest in this group and provide an efficient way to discriminate and describe species within this highly diverse genus.

In Ethiopia, overall species diversity of *Enteromius* is poorly studied and only 18 species are currently reported from the country (Dejen *et al.* 2002; Golubtsov *et al.* 2002; Getahun 2007; Habteselassie 2012; Englmaier *et al.* 2020; Prokofiev *et al.* 2021). These have generally been placed in three readily diagnosable groups (Mina *et al.* 2017): i) species with a flexible and non-serrated last unbranched ray in the dorsal fin; ii) species with a thickened and serrated last unbranched ray in the dorsal fin, and a high number of scales in the lateral series (> 32); and iii) species with a thickened and serrated last unbranched ray in the dorsal fin, a low number of scales in the lateral series (≤ 27), and a yellow, orange or reddish blotch on operculum.

Within the third group, a single population is currently known from the basins of lakes Abaya and Chamo in the Southern Main Ethiopian Rift (SMER) (Golubtsov *et al.* 2002). Occurrences from this region were last reported in 2005 and the population may be endangered due to habitat loss as a result of agricultural intensification (Mina *et al.*

2017). Morphological data of this population provided by Golubtsov & Berendzen (2005) indicate a close similarity with *E. kerstenii* (Peters, 1868). Originally described from the north-eastern coast of Tanzania (type locality given as: "Auf dem Wege von der Zanzibarküste nach dem Kilimandjàro" (Peters 1868: p. 601), translated as "on the way from the coast of Zanzibar to Kilimanjàro", and probably referring to Bagamoyo according to Greenwood (1962: p. 169)), *E. kerstenii* is thought to be widely distributed in central, eastern, and southern Africa with its northernmost limit in Ethiopia (Greenwood 1962; Skelton 2001; Golubtsov *et al.* 2002; Seegers *et al.* 2003) (**Figure 1**). Based on the last comprehensive taxonomic revision of this group by Greenwood (1962), five nominal species are currently in synonymy with *E. kerstenii* (see Seegers *et al.* 2003; Hayes & Armbruster 2017). These comprise (type locality drainage in parentheses): *E. akeleyi* (Hubbs, 1918) (Athi River, Kenya), *E. lumiensis* (Boulenger, 1903) (Lumi River, Tanzania), *E. minchini* (Boulenger, 1906) (Lake Victoria, Uganda), *E. nigrolinea* (Pfeffer, 1889) (Rufu [= Pangani] River, Tanzania), and *E. salmo* (Pfeffer, 1896) (Pangani River, Tanzania). However, morphological variability described by Greenwood (1962) and considerable genetic divergence between geographically distinct populations of *E. kerstenii* from Kenya and adjacent areas suggest unrecognized diversity in this group (Schmidt *et al.* 2017).
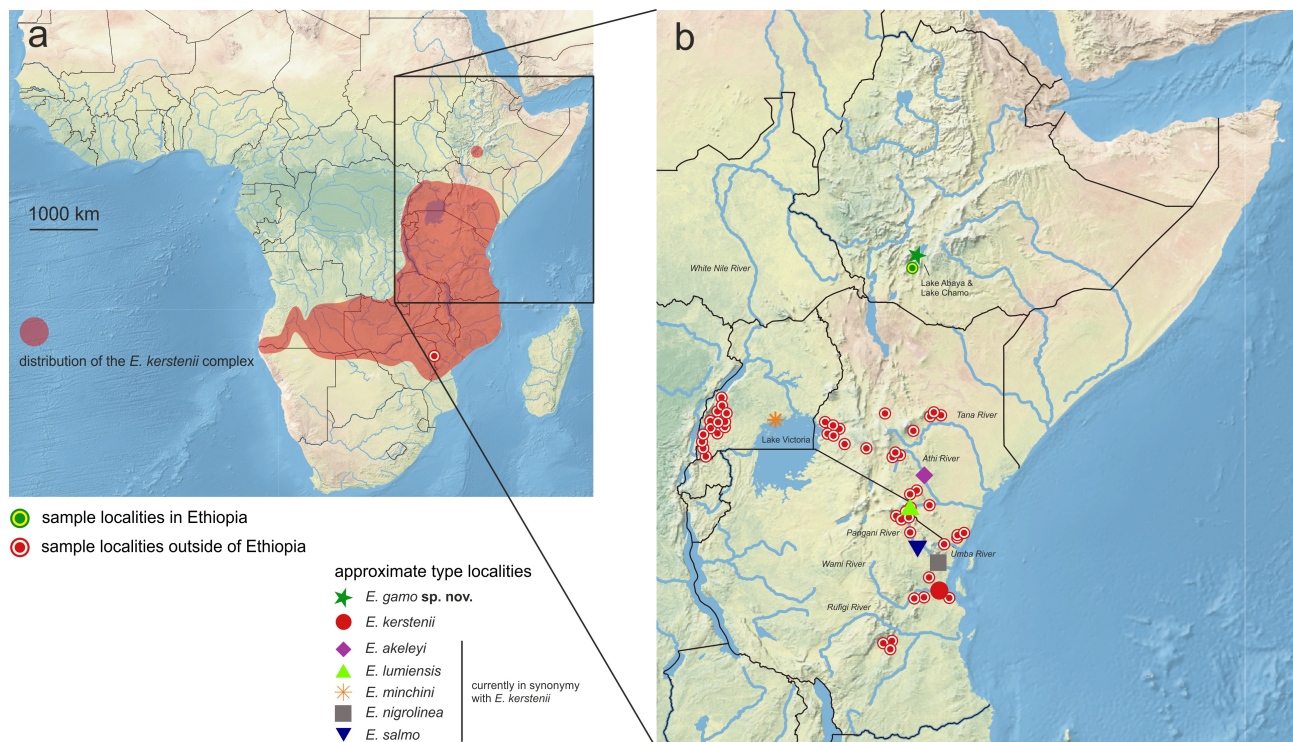

FIGURE 1. Map of the study area; **a** schematic distribution range of the *Enteromius kerstenii* complex (based on Skelton 2001; Schmidt *et al.* 2017); **b** sampling sites in the basins of lakes Abaya and Chamo in the Southern Main Ethiopian Rift and localities of comparative material in genetic and morphological analysis.

During recent field work, specimens of *E. kerstenii*-like fishes (group iii, as defined above) were re-sampled from two sites in the basins of lakes Abaya and Chamo. Here, we present new genetic and morphological data for the specimens from the SMER in comparison with the type and/or non-type material of *E. kerstenii*, *E. akeleyi*, *E. lumiensis*, *E. minchini*, *E. nigrolinea*, and *E. salmo* from Tanzania, Kenya, and Uganda in order to re-evaluate the taxonomic status of the Ethiopian population, and provide new insights into the so-called *E. kerstenii* complex (hereafter referred to simply as *E. kerstenii*).

Materials and methods

Sampling and preservation

Specimens of *Enteromius* were collected at the end of the rainy season in November 2023. Collections were made from wetlands and irrigation channels connected with tributaries of lakes Abaya and Chamo using frame nets

(mesh size 5 mm). Fish specimens were euthanised with clove oil (*Eugenia caryophyllata*) solution, fixed in 6 % pH-neutral formalin, and transferred to 75 % ethanol for long-term storage (or fixed directly in 95 % ethanol). Voucher specimens collected for the present study were deposited in the Zoological Natural History Museum, Addis Ababa, Ethiopia (ZNHM). Comparative museum samples included specimens deposited in the collections of the British Museum of Natural History (BMNH) and the Museum für Naturkunde, Leibniz-Institut für Evolutions- und Biodiversitätsforschung, Berlin, Germany (ZMB) (**Supplementary material: Table S1**).

Molecular analyses

Whole-genomic DNA was extracted from ethanol preserved fin clips using the QIAamp DNA Mini and Blood Mini Kit (QIAGEN). DNA concentrations were measured with the Qubit Broad Range Kit (Thermo Fisher Scientific).

Partial sequences of the mtDNA genes cytochrome *c* oxidase I (COI) and cytochrome *b* (cytb) were amplified for seven specimens using the primer combinations described in Behrens-Chapuis *et al.* (2015) and Bergsten *et al.* (2014), respectively. PCRs comprised 1 μl of template DNA in a 25 μl reaction volume containing 0.5 μl of each primer (10 μM), 12.5 μl of Multiplex PCR Master Mix (QIAGEN) and 10.5 μl H_2O. The thermocycling profile was set at 94°C for 3 min (initial denaturation), followed by 40 cycles of 94°C for 30 sec, 56°C for 30 sec, 72°C for 90 sec, and a final extension at 72°C for 10 min. The PCR products were purified using the PCR Purification Kit (QIAGEN), and sent to Microsynth (Balgach, Switzerland) for bi-directional sequencing using PCR primers. Sequences were edited in Chromas v.2.6.6 (https://technelysium.com.au/wp/) and aligned in MEGA v.11.0.11 (Tamura *et al.* 2021). Newly obtained sequences were deposited in the NCBI GenBank nucleotide database (https://www.ncbi.nlm.nih.gov/nucleotide/) under accession numbers PP960553–PP960559 (COI) and PP965671–PP965677 (cytb) (**Supplementary material: Table S1**).

Two different datasets were used for subsequent analyses. The first dataset comprised seven original COI sequences from Ethiopia and 58 COI sequences of *E. kerstenii* from Zimbabwe, Tanzania, and Uganda retrieved from GenBank. All sequences had a final length of 615 bp, except of three specimens from Zimbabwe (OL311874–OL311876) with 545 bp, and one specimen from Tanzania (KT199320) with 611 bp. The second dataset included seven original cytb sequences from Ethiopia and 26 cytb sequences of *E. kerstenii* from Tanzania and Kenya with a final length of 1,106 bp. Specimens of *E. kerstenii* identified by Schmidt *et al.* (2017) as introgressed with mitochondrial DNA of *E. neumayeri* (Fischer, 1884) or *E. nyanzae* (Whitehead, 1960) were not considered. Sequences of *E. paludinosus* (Peters, 1852) were used as outgroups (**Supplementary material: Table S1**).

Maximum Likelihood (ML) and Bayesian Inference (BI) approaches were used for phylogenetic inference. The best-fit nucleotide substitution model (HKY+F+G4) was identified using ModelFinder (Kalyaanamoorthy *et al.* 2017) based on the Bayesian Information Criterion. ML was performed with IQ-TREE v.1.6.8 (Nguyen *et al.* 2015) in PhyloSuite v.1.2.2 (Zhang *et al.* 2020) using 1,000 standard bootstrap replicates. For BI, MrBayes v.3.2.6 (Ronquist *et al.* 2012) was used in PhyloSuite. Two independent Markov Chain Monte Carlo (MCMC) were run simultaneously for 5 million generations with sampling trees every 500 generations. Effective sample size values (ESS) were assessed in Tracer v.1.7.1 (Rambaut *et al.* 2018), and the first 25 % of obtained trees were discarded as 'burn-in'. All trees were visualised with FigTree v.1.4.4 (Rambaut 2018). Pairwise distances (uncorrected p-distances, pairwise deletion of missing data) were calculated using MEGA v.11.0.11.

Morphological analyses

Morphometric measurements (24), meristic counts (25, including six axial skeleton counts), and two coded qualitative characters were taken from 105 specimens, following the characters summarised in Englmaier *et al.* (2020) (**Supplementary material: Table S2**). Measurements were made point-to-point using callipers to the nearest 0.1 mm. Standard length (SL) is measured from the anteriormost point of the head to the posterior margin of the hypurals at midline. The length of the penultimate unbranched dorsal fin ray is measured from radiographs, referring to a distance from the base of the ray to its tip. Counts of dorsal and anal fin rays follow Skelton (1980), with the posterior two branched rays, located on the last complex proximal pterygiophore of the fins, counted as two. All vertebral counts were made from radiographs. The first true caudal vertebra is considered as a vertebra with a "fully

developed haemal spine", i.e. similar in length to the haemal spine of the vertebra behind it. Coded lengths of the anterior and posterior barbels follow Lévêque *et al.* (1987), referring to a distance relative to the eye: 1—barbel not reaching anterior margin of the eye, 2—barbel extending between anterior margin of the eye and the middle of the eye, 3—barbel extending between the middle of the eye and the posterior margin of the eye, and 4—barbel extending beyond posterior margin of the eye.

For multivariate statistical analyses, we used principal component analysis (PCA) and analysed morphometric (24 proportional morphometric measurements and two coded characters) and meristic (25 counts) data separately. Statistical analyses were performed in Past v.4.11 (Hammer *et al.* 2001). In some specimens, measurements or counts could not be obtained due to damage. To keep these specimens in the analyses, group means (by drainage system) were used to substitute this missing data (**Supplementary material: Table S3**).

Results

Molecular analyses

Specimens from Ethiopia were resolved as a distinct lineage based on both COI (Bayesian posterior probability, BPP 1.00; bootstrap value, bs 100) and cytb (BPP 1.00; bs 100) data (**Figure 2**). Pairwise distances between the Ethiopian population and *E. kerstenii* from north-eastern Tanzania (Umba River, Pangani River, Wami River), representing localities geographically closest to the type locality of *E. kerstenii*, were 7.5–8.3 % (COI) and 8.9–10.1 % (cytb) (**Supplementary material: Tables S4–S5**). High levels of divergence were observed between geographically distinct *E. kerstenii* from Tanzania, Kenya, Uganda, and Zimbabwe. Most specimens from coastal drainages in Tanzania (Umba River, Pangani River, Wami River) and Kenya (Athi River, Tana River) were inferred as a well-supported clade based on cytb data (BPP 1.00; bs 96). Only two specimens from the Athi River (KX178168, KX178169) and one specimen from the Wami River (KX178187) were distinct from this group (**Figure 2**). Specimens from the Upper White Nile drainage in Uganda, representing the central part of the Albertine Rift, formed a weakly supported clade (BPP 0.64) based on COI data. This clade was 5.5–6.7 % divergent from the Ethiopian population.

Morphological analyses

Based on PCA, all Ethiopian specimens were well-separated from type specimens of *E. kerstenii*, *E. lumiensis*, *E. minchini*, and *E. salmo* (**Figure 3**). Morphometric data allowed clear differentiation between specimens from Ethiopia and from other localities in East Africa. Variables that contributed most to discrimination between these groups were anterior barbel length (% of snout length), posterior barbel length (% of snout length), horizontal eye diameter (% of snout length), interorbital width (% of snout length), and lower-jaw length (% of snout length) (**Table 1**). Meristic data were more similar among specimens examined. Differences were mainly observed in the number of scales in the lateral series and the number of serrae on last unbranched dorsal fin ray. The latter primarily separating the holotype of *E. salmo*, with the highest number of serrae (35), from other specimens along PC1 (**Figure 3b**).

TABLE 1. Component loadings from principal component analyses (PCA) for morphometric (24 proportional morphometric measurements and two coded characters) and meristic (25 counts) data. Bolded values contributing most variation along PC1 and PC2.

Morphometric PCA	Component Loadings		Meristic PCA	Component Loadings	
	PC1	PC2		PC1	PC2
Body depth at pelvic-fin origin (% SL)	-0.01110	-0.02504	Number of unbranched dorsal fin rays	-0.00494	-0.00333
Minimum caudal-peduncle depth (% SL)	-0.00126	-0.00534	Number of branched dorsal fin rays	0.00102	-0.00263
Caudal-peduncle length (% SL)	-0.00182	0.01868	Number of unbranched anal fin rays	0.00183	-0.00132

TABLE 1. (Continued)

| Morphometric PCA	Component Loadings		Meristic PCA	Component Loadings	
	PC1	PC2		PC1	PC2
Predorsal length (% SL)	0.01074	-0.02707	Number of branched anal fin rays	-0.00000	0.00000
Prepelvic length (% SL)	-0.00003	-0.02148	Number of unbranched pelvic fin rays	-0.00000	0.00000
Preanal length (% SL)	0.00447	-0.04411	Number of branched pelvic fin rays	-0.00045	-0.00081
Pelvic-fin length (% SL)	0.00539	0.00306	Number of unbranched pectoral fin rays	-0.00000	0.00000
Pectoral-fin length (% SL)	0.01981	-0.00255	Number of branched pectoral fin rays	0.02198	-0.02553
Head length (% SL)	-0.00032	0.01376	Number of principal caudal fin rays upper lobe	-0.00221	-0.01519
Head depth at nape (% SL)	-0.00541	0.00166	Number of principal caudal fin rays lower lobe	0.00159	0.00327
Head depth at nape (% head length)	-0.01841	-0.02974	Number of upper caudal fin procurrent rays	0.01545	-0.02789
Snout length (% head length)	-0.01267	-0.09664	Number of lower caudal fin procurrent rays	0.00445	-0.03122
Horizontal eye diameter (% head length)	0.02212	0.07435	Total number of lateral series scales	**-0.12362**	**0.71332**
Interorbital width (% head length)	-0.01917	0.04035	Number of lateral series scales to posterior margin of hypurals	**-0.10271**	**0.63111**
Horizontal eye diameter (% snout length)	**0.12588**	**0.57890**	Number of scale rows between lateral line and dorsal-fin origin	0.00200	0.00224
Interorbital width (% snout length)	-0.00350	**0.57847**	Number of scale rows between lateral line and pelvic-fin base	-0.02574	0.09864
Lower-jaw length (% snout length)	0.01362	**0.41191**	Number of scale rows between lateral line and anus	-0.02113	0.09451
Anterior barbel length (% snout length)	**0.72033**	-0.21578	Number of circumpeduncular scales	-0.00214	0.11260
Posterior barbel length (% snout length)	**0.67790**	0.11055	Total number of vertebrae	-0.02063	0.07663
Minimum caudal-peduncle depth (% caudal-peduncle length)	0.00131	-0.08349	Number of abdominal vertebrae	-0.01542	0.09159
Axillary-scale length (% pelvic-fin length)	-0.03284	-0.02034	Number of caudal vertebrae	0.00139	-0.02924
Length of lower non-serrated part of last unbranched dorsal fin ray (% length of non-segmented part of last unbranched dorsal fin ray)	-0.00273	0.18721	Number of predorsal abdominal vertebrae	-0.02125	0.07794
Length of upper serrated part of last unbranched dorsal fin ray (% length of non-segmented part of last unbranched dorsal fin ray)	0.00273	-0.18721	Number of preanal caudal vertebrae	-0.01705	0.04233
Length of penultimate unbranched dorsal fin ray (% length of non-segmented part of last unbranched dorsal fin ray)	0.04554	0.05008	Number of vertebrae between first pterygiophores of dorsal and anal fins	-0.00228	0.08958
Anterior barbel coded length	0.01347	-0.00593	Number of serrae on last unbranched dorsal fin ray	**0.98532**	**0.16692**
Posterior barbel coded length	0.01094	-0.00626			
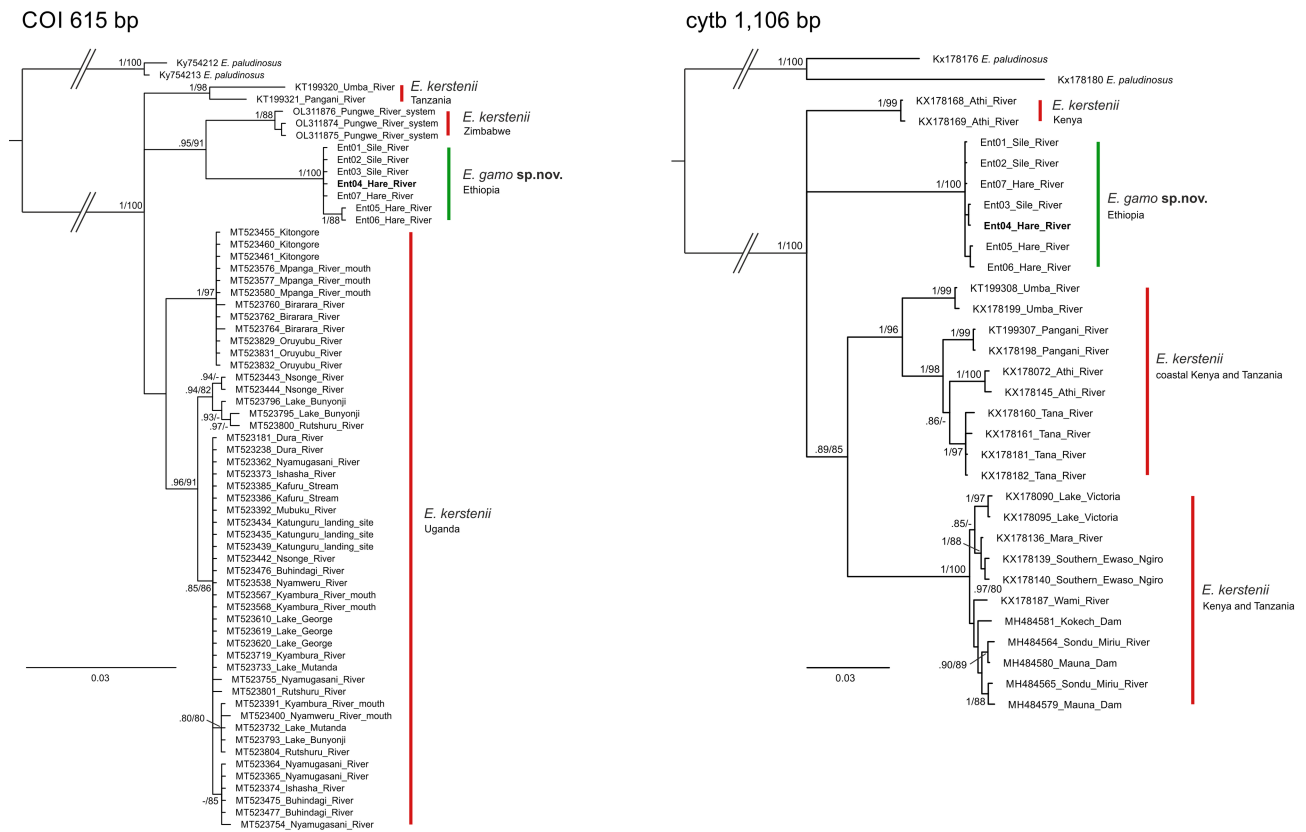
FIGURE 2. Bayesian Inference (BI) trees based on mitochondrial COI and cytb data, showing phylogenetic relationships within the *Enteromius kerstenii* complex from Ethiopia, Kenya, Tanzania, Uganda, and Zimbabwe. Node support values represent Bayesian posterior probability of BI/bootstrap values of Maximum Likelihood. Only values above .80/80 are shown. Specimens from the Umba, Pangani, and Wami rivers representing localities closest to the type locality of *E. kerstenii*; Ent04 representing the holotype of *E. gamo* **sp. nov**.
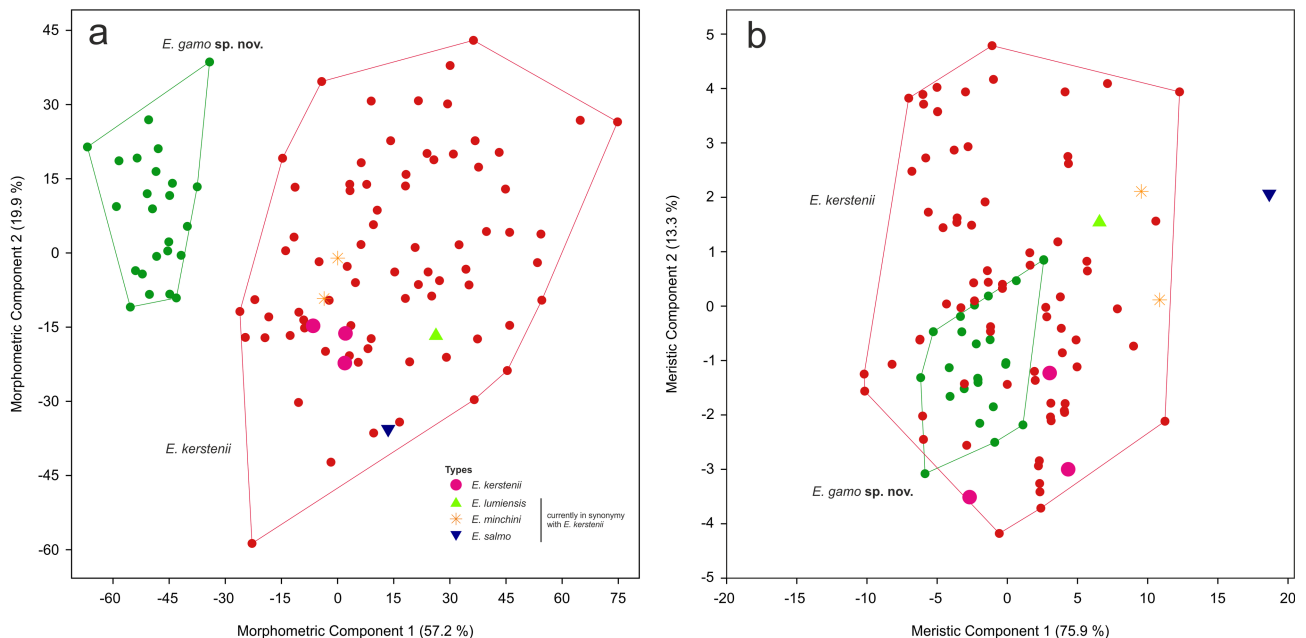

FIGURE 3. Results of PCA based on **a** 24 proportional morphometric measurements and two coded characters and **b** 25 meristic counts, comparing specimens of *Enteromius* from the basins of lakes Abaya and Chamo with type specimens of *E. kerstenii*, *E. lumiensis*, *E. minchini*, and *E. salmo* (indicated by large symbols), and non-type specimens of *E. kerstinii* from localities in Tanzania, Kenya, and Uganda.

In summary, both genetic and morphological data provide solid support to consider the Ethiopian population of *Enteromius* from the SMER (basins of lakes Abaya and Chamo), with a thickened and serrated last unbranched ray in the dorsal fin, a low number of scales in the lateral series (≤ 27), and a yellow or orange blotch on operculum, as a distinct species described below. The new species is known only from the basins of lakes Abaya and Chamo in the SMER, geographically isolated from the main distribution range of *E. kerstenii* as given in **Figure 1**.

Taxonomy

Enteromius gamo **sp. nov.**
urn:lsid:zoobank.org:act:9686B7D0-FA40-4C78-A33B-4FC44F35E391
Figure 4

Material examined. Holotype (Figure 4b). ZNHM 0080, holotype, 40.0 mm SL, irrigation channel in the floodplain of the Lower Hare River (6°3'35''N, 37°36'2''E; 1,185 m a.s.l.), Lake Abaya basin, South Ethiopia Regional State, Ethiopia, 22.11.2023, coll. G.K. Englmaier and A. Wubie, GenBank accessions PP960556 (COI) and PP965674 (cytb).

Paratypes. ZNHM 0081, 12, 30.8–44.7 mm SL, same date and locality as holotype. ZNHM 0082, 3, 35.9–37.9 mm SL, same date and locality as holotype, GenBank accessions PP960557–PP960559 (COI) and PP965675–PP965677 (cytb). ZNHM 0085, 4, 21.7–39.3 mm SL, irrigation channel connected to the Lower Sile River (5°53'31''N, 37°29'44''E; 1,122 m a.s.l.), Lake Chamo basin, South Ethiopia Regional State, Ethiopia, 19.11.2023, coll. G.K. Englmaier and A. Wubie. ZNHM 0084, 1, 34.1 mm SL, same locality as ZNHM 0085, 20.11.2023, coll. G.K. Englmaier and A. Wubie. ZNHM 0083, 3, 28.7–36.5 mm SL, same date and locality as ZNHM 0085, GenBank accessions PP960553–PP960555 (COI) and PP965671–PP965673 (cytb).

Diagnosis. *Enteromius gamo* **sp. nov.** belongs to a phenotypic group characterised by a thickened and serrated last unbranched dorsal fin ray, a low number of scales in the lateral series (≤ 27), and a yellow, orange or reddish blotch on operculum. The new species is distinguished from *E. kerstenii* and all examined congeners from Tanzania, Kenya, and Uganda primarily by short anterior (15.8–35.1 % of snout length, not reaching anterior margin of the eye) and posterior (63.2–95.7 % of snout length, extending between the middle of the eye and the posterior margin of the eye) barbels. It further differs by a short predorsal length, 49.6–56.3 % of SL; short pelvic-fin length, 16.9–20.7 % of SL, not reaching to anal-fin origin; short pectoral-fin length, 17.4–21.2 % of SL, not reaching to pelvic-fin origin; few, 14–15, branched pectoral-fin rays; few, 11, circumpeduncular scales, and few, 10–19 serrae on posterior margin of last unbranched dorsal fin ray.

Description. General appearance of *E. gamo* **sp. nov.** shown in **Figure 4**, and relative measurements, meristic counts, and coded characters of the holotype and paratypes are given in **Table 2** and **Supplementary material: Table S3**.

TABLE 2. Morphometric measurements and meristic counts for *Enteromius gamo* **sp. nov.** (ZNHM 0080, holotype; ZNHM 0081–ZNHM 0085, paratypes), and type specimens of *E. kerstenii* (ZMB 6818, lectotype; ZMB 32378 paralectotypes).

Character states	*E. gamo* sp. nov., ZNHM 0080, holotype	*E. gamo* sp. nov., holotype and paratypes					*E. kerstenii*, ZMB 6818, lectotype	*E. kerstenii*, lectotype and paralectotypes				
		n	Min	Max	Mean	S.D.		n	Min	Max	Mean	S.D.
Standard length (mm)	40.0	24	21.7	44.7	35.0	5.0	62.8	3	46.7	62.8	54.6	8.1
MORPHOMETRIC DATA												
Percent of standard length												
Body depth at pelvic-fin origin	32.5	24	24.8	32.9	29.9	1.9	33.4	3	28.1	33.4	30.1	2.9
Caudal-peduncle length	21.3	24	19.7	23.3	21.6	0.9	20.2	3	20.2	21.0	20.5	0.4

......continued on the next page

TABLE 2. (Continued)

Character states	E. gamo sp. nov., ZNHM 0080, holotype	E. gamo sp. nov., holotype and paratypes					E. kerstenii, ZMB 6818, lectotype	E. kerstenii, lectotype and paralectotypes				
		n	Min	Max	Mean	S.D.		n	Min	Max	Mean	S.D.
Minimum caudal-peduncle depth	14.5	24	13.2	14.8	14.0	0.5	15.0	3	12.9	15.0	13.9	1.0
Predorsal length	56.3	24	49.6	56.3	51.8	1.5	54.6	3	53.0	54.6	53.9	0.9
Prepelvic length	49.5	24	48.4	51.7	49.9	0.9	52.5	3	49.1	52.5	50.7	1.7
Preanal length	71.3	24	68.3	73.0	70.9	1.1	76.9	3	72.9	76.9	74.8	2.0
Dorsal-fin depth	27.5	24	24.4	31.5	28.6	1.9	21.7	3	21.7	26.1	24.2	2.4
Anal-fin depth	18.3	24	17.9	21.2	19.5	0.9	18.6	3	16.2	19.7	18.2	1.8
Pelvic-fin length	18.3	24	16.9	20.7	18.6	1.0	21.5	3	20.3	21.5	20.6	1.0
Pectoral-fin length	18.3	24	17.4	21.2	19.5	1.1	22.9	3	22.3	23.1	22.8	1.1
Head length	27.8	24	26.6	29.6	28.0	0.9	29.8	3	26.0	29.8	28.0	1.9
Head depth at nape	20.3	24	18.9	20.8	20.0	0.5	20.4	3	19.2	20.4	19.8	0.6
Percent of caudal-peduncle length												
Minimum caudal-peduncle depth	68.2	24	58.3	72.7	64.8	4.1	74.0	3	63.6	74.0	68.0	5.4
Anal-fin depth	85.9	24	81.0	102.7	90.5	6.3	92.1	3	80.0	93.9	88.7	7.6
Percent of head length												
Head depth at nape	73.0	24	67.0	74.5	71.4	2.2	68.5	3	68.5	73.8	70.9	2.7
Snout length	30.6	24	26.4	30.8	29.1	1.2	31.6	3	30.3	31.6	30.8	0.7
Horizontal eye diameter	26.1	24	24.5	34.9	28.4	2.4	32.1	3	29.1	32.1	30.5	1.5
Interorbital width	43.2	24	36.3	47.6	41.5	2.6	38.0	3	34.8	38.0	35.9	1.8
Percent of snout length												
Horizontal eye diameter	85.3	24	83.3	117.4	97.9	10.1	101.7	3	95.4	101.7	99.1	3.3
Interorbital width	141.2	24	117.9	169.6	143.1	11.1	120.3	3	114.0	120.3	116.4	3.4
Lower-jaw length	126.5	24	115.8	154.8	132.4	10.3	127.1	3	127.1	130.0	128.3	1.5
Anterior barbel length	32.4	24	15.8	35.1	27.4	5.9	81.4	3	75.0	81.4	78.5	3.2
Posterior barbel length	73.5	24	63.2	95.7	81.0	7.4	96.6	3	90.0	100.0	95.5	5.1
Percent of horizontal eye diameter												
Anterior barbel length	37.9	24	13.6	41.9	28.5	7.7	80.0	3	80.0	82.9	79.3	4.0
Posterior barbel length	86.2	24	54.5	100.0	83.5	10.3	95.0	3	90.0	104.9	96.3	7.6
Percent of pelvic-fin length												
Axillary-scale length	32.9	24	23.4	44.1	31.0	5.5	25.2	3	21.8	25.2	23.8	1.8
Percent of non-segmented part of last unbranched dorsal fin ray (from x-rays)												
Length of penultimate unbranched dorsal fin ray	29.6	15	26.4	38.3	32.2	3.7	39.8	3	37.9	51.7	43.1	7.5
Length of lower non-serrated part of last unbranched dorsal fin ray	39.0	15	28.5	40.3	35.3	3.8	34.1	3	32.4	40.6	35.7	4.3

TABLE 2. (Continued)

Character states	E. gamo sp. nov., ZNHM 0080, holotype	E. gamo sp. nov., holotype and paratypes					E. kerstenii, ZMB 6818, lectotype	E. kerstenii, lectotype and paralectotypes				
		n	Min	Max	Mean	S.D.		n	Min	Max	Mean	S.D.
Length of upper serrated part of last unbranched dorsal fin ray	61.0	15	59.7	71.5	64.7	3.8	65.9	3	59.4	67.6	64.3	4.3
CODED CHARACTERS												
Anterior barbel coded length	1	1(24)					2	2(3)				
Posterior barbel coded length	3	3(24)					3	3(3)				
MERISTIC DATA												
Dorsal fin rays	III-8	III-8(19)					III-8	III-8(3)				
Anal fin rays	III-6	III-6(19)					III-6	III-6(3)				
Pelvic fin rays	I-7	I-7(24)					I-7	I-7(3)				
Pectoral fin rays	I-14	I-14(16), I-15(8)					I-16	I-15(2), I-16(1)				
Caudal-fin principal rays (upper lobe + lower lobe)	9+8	9+8(16), 10+8(1)					9+8	9+8(3)				
Caudal-fin procurrent rays (upper + lower)	8+7	8+7(11), 8+8(1), 9+8(2)					9+8	9+8(2), 10+8(1)				
Total number of lateral series scales	27	25(5), 26(11), 27(8)					24	24(2), 25(1)				
Lateral series scales to posterior margin of hypurals	25	23(3), 24(9), 25(12)					22	22(1), 23(1), 24(1)				
Scale rows between lateral line and dorsal-fin origin	5	5(24)					5	5(3)				
Scale rows between lateral line and pelvic-fin base	3	3(24)					3	3(3)				
Scale rows between lateral line and anus	3	3(24)					3	3(3)				
Circumpeduncular scales	11	11(24)					12	12(3)				
Total number of vertebrae	33	32(1), 33(13), 34(6)					33	33(3)				
Abdominal vertebrae	18	17(1), 18(18), 19(1)					18	18(3)				
Caudal vertebrae	15	15(15), 16(5)					15	15(3)				
Predorsal abdominal vertebrae	10	8(1), 9(6), 10(13)					9	9(2), 10(1)				
Preanal caudal vertebrae	0	0(20)					0	0(3)				
Vertebrae between first pterygiophores of dorsal and anal fins	8	7(3), 8(13), 9(4)					9	8(1), 9(2)				

TABLE 2. (Continued)

Character states	*E. gamo* sp. nov., ZNHM 0080, holotype	*E. gamo* sp. nov., holotype and paratypes					*E. kerstenii*, ZMB 6818, lectotype	*E. kerstenii*, lectotype and paralectotypes				
		n	Min	Max	Mean	S.D.		n	Min	Max	Mean	S.D.
Supraneural bones	6			5(2), 6(3)			5			5(3)		
Serrae on last unbranched dorsal fin ray	15			10(2), 11(1), 12(2), 13(3), 14(1), 15(4), 16(2), 17(2), 19(2)			20			13(1), 19(1), 20(1)		
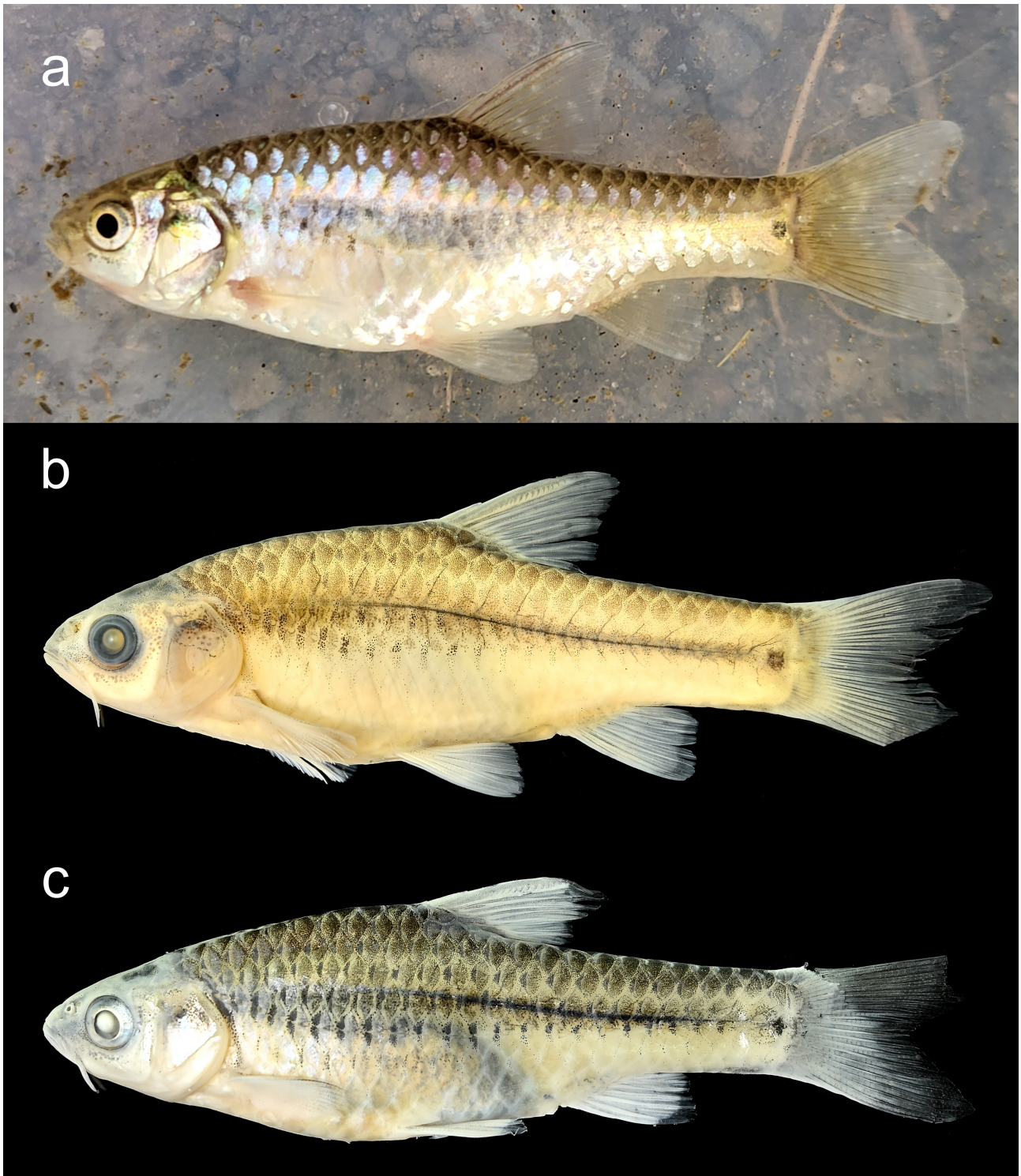
FIGURE 4. General appearance of *Enteromius gamo* **sp. nov.** from the lower Sile and Hare rivers; **a** live specimen, ZNHM 0082, paratype, 36.7 mm SL; **b** ZNHM 0080, holotype, 40.0 mm SL; **c** ZNHM 0083, paratype, 36.5 mm SL.

Longest examined specimen 44.7 mm SL (ZNHM 0081). Body moderately compressed. Dorsal head profile and predorsal back straight or slightly concave. Postdorsal back outline slightly convex to end of caudal peduncle. Head usually shorter than body depth at pelvic-fin origin. Snout rounded; its length usually slightly greater than horizontal eye diameter. Mouth terminal, tip of mouth cleft slightly lower than level of middle of eye, mouth cleft straight. Anterior barbel short (15.8–35.1 % of snout length) not reaching anterior margin of the eye (coded length 1). Posterior barbel 63.2–95.7 % of snout length, extending between the middle of the eye and the posterior margin of the eye (coded length 3), never reaching beyond posterior margin of the eye. Eye large, but horizontal diameter usually smaller than snout length. Eye diameter relative to snout length negatively correlated with SL (R = -0.80 Spearman's rank correlation, N = 24). Interorbital width greater than horizontal eye diameter.

Dorsal fin with three unbranched and eight branched rays. Last unbranched ray thickened and densely serrated on posterior margin. Serration extending over 60–72 % (mean 65 %) of non-segmented part, lower non-serrated part relatively short. Number of serrae ranging from 10 (28.7 mm SL) to 19 (44.7 mm SL), but not positively correlated with size (R = 0.44, Spearman's rank correlation, N = 19). Dorsal-fin origin usually behind origin of pelvic fin. Dorsal-fin depth usually slightly longer than head length. Anal fin with three unbranched and six branched rays, reaching to about middle of caudal peduncle; depth 81.0–102.7 % of caudal-peduncle length. Pelvic fin with one unbranched and seven branched rays, not reaching to anal-fin origin. Pectoral fin with one unbranched and 14 or 15 branched rays, not reaching pelvic-fin origin. Pectoral and anal fins of about similar length, pelvic fin commonly shorter. Caudal fin forked with typically 2+17 principal rays (nine in upper lobe and eight in lower lobe). Upper procurrent rays eight or nine, lower procurrent rays seven or eight (**Table 2**).

Lateral line complete and downwardly curved below midline, running along midline on caudal peduncle. Total number of scales in the lateral series 25–27, mode 26. Scale rows between lateral line and dorsal-fin origin five, three scale rows between lateral line and pelvic-fin base as well as between lateral line and anus. Circumpeduncular scale rows 11. Back, belly and chest fully scaled. Axillary scale present at pelvic-fin base; length 23.4–44.1 % of pelvic-fin length.

Total vertebrae 32–34, commonly 33; with 17–19 abdominal vertebrae and 15–16 caudal vertebrae; predorsal abdominal vertebrae 8–10, mode 10, other vertebral counts given in **Table 2**. Supraneurals five or six (N = 6), first two or three roundish and three or four in front of dorsal fin deeper and elongated.

Gill rakers in outer row of first gill arch 43–45 (N = 3), with 28 or 29 on lower limb and 14, 15, or 17 on upper limb.

In three examined specimens (39.3–41.9 mm SL), length of digestive tract (straightened but not stretched) about 78–81 % of SL. Intestine folded in simple loop before reaching anus.

Mature spawning capable females with large ovaries, i.e. the developing phase of the reproductive cycle (Brown-Peterson *et al.* 2011), were observed end of rainy season at sizes of 39.3–41.9 mm SL (N = 3).

Colouration. In life (**Figure 4a**), body silvery or cream-coloured, darker above lateral line with black or brownish back. Blueish, yellowish or orange iridescent above lateral line in anterior half of body, on operculum, and upper eye. Yellow or orange blotch on operculum. Small, distinct black spot at posterior margin of caudal peduncle. Fins pale, base of caudal fin cream-coloured or yellowish.

In formalin (initial fixation) and later transferred to 75 % ethanol specimens (**Figure 4b**), pale cream-coloured. Upper head ash-grey. Back with greyish or black stripe. Faint greyish stripe between anal-fin insertion and caudal fin. Narrow black mid-lateral stripe, most prominent between level of pelvic-fin origin and level of anal-fin insertion, terminating in a small black spot at posterior margin of caudal peduncle. Scales above mid-lateral stripe with abundant, small, and uniformly distributed dark pigments. Concentration of dark pigments at anterior border of pored scales forming chevrons, most distinct anterior to dorsal-fin origin. Small dark brown or black blotch on operculum. Fins white.

Ethanol-preserved specimens (**Figure 4c**), overall cream-coloured and greyish above lateral line, with darker back, and with observable shine at midline and operculum. Narrow black mid-lateral stripe and faint greyish stripe between anal-fin insertion and caudal fin present. Pigmentation of scales similar to specimens initially preserved in formalin, but darker and more intense. Small black spot at posterior margin of caudal peduncle. Fins pale or greyish.

Distribution and habitat. *Enteromius gamo* **sp. nov.** is endemic to Ethiopia where it is known only from the endorheic basins of lakes Abaya and Chamo in the SMER. The new species was collected at the end of the rainy season from irrigation channels connected to the lower Sile and Hare rivers with their associated floodplains

(**Figure 5**). In both sampling sites, *E. gamo* **sp. nov.** was found sympatric with *Enteromius* cf. *stigmatopygus*. Substrate composition was dominated by silt and sand. The altitude of the sampling sites ranged from 1,122 m a.s.l. (5°53'31''N, 37°29'44''E) to 1,185 m a.s.l. (6°3'35''N, 37°36'2''E). *Enteromius gamo* **sp. nov.** was absent from mainstem rivers and only a single specimen was previously found in littoral habitats of Lake Abaya (Golubtsov *et al.* 2002). Additionally, the new species was reported from the Sago River, Lake Chamo basin (Golubtsov *et al.* 2002).

FIGURE 5. Habitat of *Enteromius gamo* **sp. nov.** in the lower Sile and Hare rivers; **a** irrigation channel and associated wetland in the floodplain of the Lower Hare River (6°3'35''N, 37°36'2''E; 1,185 m a.s.l.), Lake Abaya basin, type locality of *E. gamo* **sp. nov.**; **b** irrigation channel connected to the Lower Sile River (5°53'31''N, 37°29'44''E; 1,122 m a.s.l.), Lake Chamo basin.

Gut contents examined ($N = 3$) contained unidentifiable fine organic detritus, remains of aquatic (Chironomidae, Ephemeroptera) and terrestrial (Formicidae) arthropods, and some non-organic material (sand grains).

Etymology. The specific epithet *gamo* was selected in honour of the Gamo people, who inhabit the region around Lake Abaya where the holotype was collected. A noun.

Remarks. The restricted distribution range of *E. gamo* **sp. nov.** coupled with environmental pressures from agricultural intensification and subsequent modification of the natural habitat suggest that the new species should be listed with an IUCN (2012) status of Endangered or Critically Endangered.

Comparison of *Enteromius gamo* sp. nov. with East African congeners. Besides the main diagnostic characters mentioned above, the newly described species from Ethiopia differs clearly from type specimens of *E. kerstenii* (**Figure 6a**, **Table 2**) by 14–15, mode 14, branched pectoral fin rays (vs. 15–16); 25–27, mode 26, scales in the lateral series (vs. 24–25); length of penultimate unbranched dorsal fin ray 26.4–38.3 %, mean 32.2 %, of non-segmented length of last unbranched dorsal fin ray (vs. 37.9–51.7 %, mean 43.1 %, of non-segmented length of last unbranched dorsal fin ray); axillary scale 23.4–44.1 %, mean 31.0 %, of pelvic-fin length (vs. 21.8–25.2 %, mean 23.8 %, of pelvic-fin length); and interorbital width 117.9–169.6 %, mean 143.1 %, of snout length (vs. 114.0–120.3 %, mean 116.4 %, of snout length).

Enteromius gamo **sp. nov.** is distinguished from the holotype of *E. lumiensis* (**Figure 6b**), originating from the Lumi River, a tributary to Lake Jipe on the east side of Mount Kilimanjaro (north-eastern Tanzania), by 14–15, mode 14, branched pectoral fin rays (vs. 15); horizontal eye diameter 83.3–117.4 %, mean 97.9 %, of snout length (vs. 82.4 % of snout length); and minimum caudal-peduncle depth 58.3–72.7 %, mean 64.8 %, of caudal-peduncle length (vs. 61.1 % of caudal-peduncle length).

No type material of *E. nigrolinea*, originating from the Pangani River (historically referred to as "Rufu River" in its middle course), was examined and we refer to published data (original description by Pfeffer 1889) for comparison. *Enteromius gamo* **sp. nov.** is distinguished from *E. nigrolinea* by body depth greater than head length (vs. equal); eye diameter shorter than snout length (vs. longer); and interorbital width considerably shorter than twice eye diameter (vs. almost equal to twice eye diameter). The new species also differs from the holotype of *E. salmo* (**Figure 6c**), described from the Pangani River, by 10–19, mode 15, serrae on last unbranched dorsal fin ray (vs. 35); and horizontal eye diameter 83.8–117.4 %, mean 97.9 %, of snout length (vs. 77.4 % of snout length).

FIGURE 6. General appearance of **a** ZMB 6818, *Enteromius kerstenii*, lectotype, 62.8 mm SL, "Auf dem Wege von der Zanzibarküste nach dem Kilimandjàro" (Peters 1868: p. 601), Tanzania, photograph: E. Aßel; **b** BMNH 1902.11.8.21, *E. lumiensis*, holotype, 59.2 mm SL, Lumi River, eastern side of Kilimanjaro, running into Lake Jipi, Tanzania, photograph: © The Trustees of the Natural History Museum, London; **c** ZMB 13163, *E. salmo*, holotype, 70.9 mm SL, Pangani River, Tanzania, photograph: E. Aßel; **d** BMNH 1906.5.30.123-124, *E. minchini*, syntype, 63.9 mm SL, Entebbe, Lake Victoria, Uganda, photograph: © The Trustees of the Natural History Museum, London.

FIGURE 7. General appearance of *Enteromius kerstenii* from Kenya, Tanzania, and Uganda; **a** BNMH 1975.10.7.19–31, *E. kerstenii*, 47.9 mm SL, Upper Pangani River, Tanzania; **b** *E. kerstenii*, 75.7 mm SL, Makindu & Tsavo Rivers, Athi River system, Kenya; **c** BMNH 1958.4.23.1–13, *E. kerstenii*, 56.8 mm SL, Lake Bunyoni, Uganda; **d** BNMH 1969.2.11.255–260, *E. kerstenii*, 36.7 mm SL, Kikwawira, tributary of Kilombero River, Rufiji River system, Tanzania. Photographs: © The Trustees of the Natural History Museum, London.

Additional material from the Pangani River drainage (**Figure 7a**), showed that *E. gamo* **sp. nov.** differs by length of non-segmented and serrated part of last unbranched dorsal fin ray 59.7–71.5 %, mean 64.7 %, of non-segmented length of last unbranched dorsal fin ray (vs. 66.3–77.5 %, mean 71.4 %, of non-segmented length of last unbranched dorsal fin ray). Data from COI and cytb place specimens from the Pangani River within a group of specimens from other coastal drainages in Tanzania and Kenya, divergent from *E. gamo* **sp. nov.** by 7.5–7.8 % (COI) and 9.2–9.4 % (cytb).

We did not examine type material of *E. akeleyi*, but examination of specimens from the Athi River drainage (**Figure 7b**), closest to the type locality of *E. akeleyi*, showed that they are different from *E. gamo* **sp. nov.** by 3–4, mode 4, unbranched dorsal fin rays (vs. 3); 8–10, mode 9, vertebrae between first pterygiophores of dorsal and anal fins (vs. 7–9, mode 8); and preanal length 71.0–76.7 %, mean 74.4 %, of SL (vs. 68.3–73.0 %, mean 70.9 %, of SL).

Enteromius gamo **sp. nov.** is further distinguished from *E. minchini* (Lake Victoria, **Figure 6d**) by 8–10, mode 10, predorsal abdominal vertebrae (vs. 9); and minimal caudal-peduncle depth 58.3–72.7 %, mean 64.8 %, of caudal-peduncle length (vs. 56.3–61.4 %, mean 58.8 %, of caudal-peduncle length). Specimens from Lake Bunyoni (**Figure 7c**) in the Upper White Nile are geographically closest to the type locality of *E. minchini* and distinct from *E. gamo* **sp. nov.** by 32–33, mode 32, total vertebrae (vs. 32–34, mode 33); head depth at nape 72.0–81.4 %, mean 75.4 %, of head length (vs. 67.0–74.5 %, mean 71.4 %, of head length); and body depth at pelvic-fin origin 31.0–36.5 %, mean 33.8 %, of SL (vs. 24.8–32.9 %, mean 29.9 %, of SL).

The new species is further distinguished from *E. kerstenii*-like fishes from south-eastern Tanzania (Rufiji River system) (**Figure 7d**) by 8–10, mode 10, predorsal abdominal vertebrae (vs. 9–10, mode 9); and length of penultimate unbranched dorsal fin ray 26.4–38.3 %, mean 32.2 %, of non-segmented length of last unbranched dorsal fin ray (vs. 34.2–43.0 %, mean 38.6 %, of non-segmented length of last unbranched dorsal fin ray). The number of lateral series scales largely overlaps (25–27 vs. 26–30), but the highest counts of 28–30, recorded in specimens from Rufiji, were not found in *E. gamo* **sp. nov.**

Discussion

Combined genetic and morphological data provide solid support to distinguish the Ethiopian population of *Enteromius* with a thickened and serrated last unbranched ray in the dorsal fin, a low number of scales in the lateral series (≤ 27), and a yellow or orange blotch on operculum as a new species, distinct from *E. kerstenii* and congeners from Tanzania, Kenya, and Uganda. The new species, *E. gamo* **sp. nov.**, is known only from the endorheic basins of lakes Abaya and Chamo in the SMER, representing the only endemic fish species from this region thus far. With the description of the new species, each part of the Main Ethiopian Rift (MER) harbours an endemic species of *Enteromius*—*E. yardiensis* Englmaier, Tesfaye & Bogutskaya, 2020 (Northern MER), *E. akakianus* (Boulenger, 1911) (Central MER, also in the Upper Awash River drainage but there probably extirpated), and *E. gamo* **sp. nov.** (SMER). While *E. yardiensis* and *E. akakianus* belong to the *E. pleurogramma* complex (sensu Mina *et al.* 2017; frequently misidentified as *E. paludinosus*), *E. gamo* is part of the *E. kerstenii* complex reflecting faunal similarities between the SMER and both the Nilo-Sudan and East-Coast ichthyofaunal provinces (Golubtsov & Habteselassie 2010). The last paleohydrological connection from lakes Abaya and Chamo to Lake Turkana via the Chew Bahir basin is evident during the African Humid Period (12.0–6.5 ka) (Grove *et al.* 1975; Roberts 1975 Dommain *et al.* 2022). This connection opened dispersal pathways from the White Nile system and potentially from the headwaters of rivers originating in central Kenya (Dommain *et al.* 2022) where *E. kerstenii* is currently distributed (Seegers *et al.* 2003). The timing of dispersal or vicariance is unknown but changes in paleoclimatic conditions and modifications of hydrological networks in this region occurred repeatedly within the last ~4 Ma (Nutz *et al.* 2020) with multiple events therefore potentially contributing to the distribution and subsequent isolation of fish species in the endorheic basins of the SMER (Golubtsov & Habteselassie 2010).

The newly described species from the basins of lakes Abaya and Chamo represents the northernmost distribution limit of the *E. kerstenii* complex. Otherwise this group is widely distributed in eastern, central, and southern Africa (Skelton 2001; Schmidt *et al.* 2017) and likely includes several distinct species. Additional studies will be needed to evaluate the extent of morphological and genetic differences between geographically distinct populations of *E. kerstenii*. Also, morphological similarities with *E. tangandensis* (Jubb, 1954) and *E. eutaenia* (Boulenger, 1904), as

discussed in Greenwood (1962), need further investigation. Especially the extent and variability in the mid-lateral stripe, mainly differentiating *E. tangandensis* and *E. eutaenia* from *E. kerstenii* (Greenwood 1962), is unknown.

Similar to other species complexes in the genus (e.g. Van Ginneken *et al.* 2017; Schmidt *et al.* 2018; Englmaier *et al.* 2020), the combination of genetic markers with morphometric and meristic characters, proved to be informative for species differentiation in this group. The presence of hybridization reported between *E. kerstenii* and *E. nyanzae* and between *E. kerstenii* and *E. neumayeri* in Schmidt *et al.* (2017) highlights the importance of including sequence data for historical type specimens in order to resolve the taxonomy within this group.

Acknowledgements

Data availability statement

The newly obtained mitochondrial COI and cytb sequences are available from the NCBI GenBank nucleotide database (https://www.ncbi.nlm.nih.gov/nucleotide/) under accession numbers PP960553–PP960559 (COI) and PP965671–PP965677 (cytb) (**Supplementary material: Table S1**). Morphological data are available from **Supplementary material: Table S3**. The supplementary material is available at DOI 10.6084/m9.figshare.26494624

Conflict of interest

The authors declare no conflict of interest.

References

Behrens-Chapuis, S., Herder, F., Esmaeili, H.R., Freyhof, J., Hamidan, N.A., Özuluğ, M., Šanda, R. & Geiger, M.F. (2015) Adding nuclear rhodopsin data where mitochondrial COI indicates discrepancies – can this marker help to explain conflicts in cyprinids? *DNA Barcodes*, 3, 187–199.
https://doi.org/10.1515/dna-2015-0020

Bergsten, J., Engl, M. & Ericsson, P. (2014) A DNA key to all Swedish vertebrates. Published in. GenBank. Available from: http://www.ncbi.nlm.nih.gov (accessed 19 August 2024)

Boulenger, G.A. (1903) Descriptions of Four new Species of *Barbus* discovered by Mr. A. Blayney Percival in East Africa. *Annals and Magazine of Natural History*, Series 7, 11 (61), 52–54.
https://doi.org/10.1080/00222930308678719

Boulenger, G.A. (1904) *Barbus eutaenia* and *B. holotaenia*, new names for *Barbus kessleri*, Günther *nec* Steindachner. *Annals and Magazine of Natural History*, Series 7, 14 (81), Art. 32, 218.
https://doi.org/10.1080/03745480409442997

Boulenger, G.A. (1906) Descriptions of new fishes discovered by Mr. E. Degen in Lake Victoria. *Annals and Magazine of Natural History*, Series 7, 17 (101), 433–452.
https://doi.org/10.1080/00222930608562554

Boulenger, G.A. (1911) *Catalogue of the fresh-water fishes of Africa in the British Museum (Natural History). Vol. 2* Printed by order of the Trustees [by Taylor and Francis], London, xii + 529 pp.

Brown-Peterson, N.J., Wyanski, D.M., Saborido-Rey, F., Macewicz, B.J. & Lowerre-Barbieri, S.K. (2011) A standardized terminology for describing reproductive development in fishes. *Marine and Coastal Fisheries*, 3 (1), 52–70.
https://doi.org/10.1080/19425120.2011.555724

Cope, E.D. (1867) Synopsis of the Cyprinidae of Pennsylvania. With supplement on some new species of American and African fishes. *Transactions of the American Philosophical Society*, 13, 351–410.
https://doi.org/10.2307/1005371

Dejen, E., Rutjes, H.A., De Graaf, M., Nagelkerke, L.A.J., Osse, J.W.M. & Sibbing, F.A. (2002) The 'small barbs' *Barbus humilis* and *B. trispilopleura* of Lake Tana (Ethiopia): are they ecotypes of the same species? *Environmental Biology of Fishes*, 65 (4), 373–386.
https://doi.org/10.1023/A:1021110721565

Dommain, R., Riedl, S., Olaka, L.A., deMenocal, P., Deino, A.L., Owen, R.B., Muiruri, V., Müller, J., Potts, R. & Strecker, M.R. (2022) Holocene bidirectional river system along the Kenya Rift and its influence on East African faunal exchange and diversity gradients. *Proceedings of the National Academy of Sciences*, 119 (28), e2121388119.
https://doi.org/10.1073/pnas.2121388119

Englmaier, G.K., Tesfaye, G. & Bogutskaya, N.G. (2020) A new species of *Enteromius* (Actinopterygii, Cyprinidae, Smiliogastrinae) from the Awash River, Ethiopia, and the re-establishment of *E. akakianus*. *ZooKeys*, 902, 107–150.
https://doi.org/10.3897/zookeys.902.39606

Fischer, J.G. (1884) Über einige Afrikanische Reptilien, Amphibien, und Fische des Naturhistorischen Museums. I. Über die von Herrn G. A. Fischer im Massai-Gebiete (Ost-Afrika) auf seiner in Veranlassung der Geographischen Gesellschaft in Hamburg unternommenen Expedition gesammelten Reptilen, Amphibien und Fische. *Jahrbuch der Hamburgischen Wissenschaftlichen Anstalten*, 1, 1–32, pls. 1–3. [in German]

Getahun, A. (2007) An overview of the diversity and conservation status of the Ethiopian freshwater fish fauna. *Journal of Afrotropical Zoology*, Special Issue, 87–96.

Golubtsov, A.S., Dgebuadze, Y.Y. & Mina, M.V. (2002) Fishes of the Ethiopian Rift Valley, Chapter 10. *In*: Tudorancea, C., Taylor, W.D., Baele, G. & Suchard, M.A. (Eds.) *Ethiopian Rift Valley Lakes*. Biology of Inland Waters Series. Backhuys Publishers, Leiden, pp. 167–258.

Golubtsov, A.S. & Berendzen, P.B. (2005) A review of the small barbs (*Barbus*, Cyprinidae) with a serrated dorsal spine from Ethiopia, with a discussion of the origin of forms with a reduced dorsal spine from the White Nile and Omo River tributaries. *Journal of Ichthyology*, 45 (Supplement 1), 58–88.

Golubtsova A.S. & Habteselassie, R. (2010) Fish faunas of the Chamo-Abaya and Chew Bahir basins in southern portion of the Ethiopian Rift Valley: origin and prospects for survival. *Aquatic Ecosystem Health & Management*, 13 (1), 47–55.
https://doi.org/10.1080/14634980903578506

Greenwood, P.H. (1962) A revision of certain *Barbus* (Pisces, Cyprinidae) from east, central, and south Africa. *Bulletin of the British Museum (Natural History)*, Zoology, 8 (4), 153–208.
https://doi.org/10.5962/p.118628

Grove, A.T., Street, F.A. & Goudie, A.S. (1975) Former lake levels and climatic change in the rift valley of Southern Ethiopia. *Geographical Journal*, 141 (2), 177–194.
https://doi.org/10.2307/1797205

Habteselassie, R. (2012) *Fishes of Ethiopia, Annotated Checklist with Pictorial Identification Guide, 1st Edition*. Ethiopian Fisheries and Aquatic Science Association, Addis Ababa, 250 pp.

Hammer, Ø., Harper, D.A.T. & Ryan, P.D. (2001) PAST: Paleontological statistics software package for education and data analysis. *Palaeontologia Electronica*, 4 (1), 1–9. [http://palaeo-electronica.org/2001_1/past/issue1_01.htm]

Hayes, M.M. & Armbruster, J.W. (2017) The taxonomy and relationships of the African small barbs (Cypriniformes: Cyprinidae). *Copeia*, 105 (2), 348–362.
https://doi.org/10.1643/CI-15-348

Hubbs, C.L. (1918) Notes on fishes from the Athi River in British East Africa. *Field Museum of Natural History, Publications, Zoological Series*, 12 (2), 9–16.
https://doi.org/10.5962/bhl.title.3072

IUCN (2012) *IUCN Red List Categories and Criteria: Version 3.1. 2nd Edition*. IUCN, Gland and Cambridge, iv + 32 pp.

Jubb, R.A. (1954) A note on a collection of freshwater fishes being prepared for the Queen Victoria Museum. *Occasional Papers of the National Museum of Southern Rhodesia*, 2 (19), 690–698, pl. 1.

Kalyaanamoorthy, S., Minh, B.Q., Wong, T.K.F., von Haeseler, A. & Jermiin, L.S. (2017) ModelFinder: Fast model selection for accurate phylogenetic estimates. *Nature Methods*, 14, 587–589.
https://doi.org/10.1038/nmeth.4285

Kambikambi, M.J., Kadye, W.T. & Chakona, A. (2021) Allopatric differentiation in the *Enteromius anoplus* complex in South Africa, with the revalidation of *Enteromius cernuus* and *Enteromius oraniensis*, and description of a new species, *Enteromius mandelai* (Teleostei: Cyprinidae). *Journal of Fish Biology*, 99 (3), 931–954.
https://doi.org/10.1111/jfb.14780

Kisekelwa, T., Snoeks, J., Decru, E., Schedel, F.B.D., Isumbisho, M. & Vreven, E. (2022) A mismatch between morphological and molecular data in lineages of *Enteromius* (Cypriniformes: Cyprinidae) from the Lowa basin (East Democratic Republic of the Congo: DRC) with the description of a new species. *Systematics and Biodiversity*, 20 (1), 1–22.
https://doi.org/10.1080/14772000.2022.2135630

Lévêque, C., Teugels, G.G. & Thys Van Den Audenaerde, D.F.E. (1987) Révision de quelques *Barbus* à trois taches (Pisces, Cyprinidae) d'Afrique de l'Ouest, avec la description de trois Nouvelles espèces: *B. tiekoroi* sp. n., *B. traorei* sp. n. et *B. trispiloides* sp. n. *Revue d'hydrobiologie tropicale*, 20 (2), 165–184. [in French]

Maetens, H., Van Steenberge, M., Snoeks, J. & Decru, E. (2020) Revalidation of *Enteromius alberti* and presence of *Enteromius* cf. *mimus* (Cypriniformes: Cyprinidae) in the Lake Edward system, East Africa. *European Journal of Taxonomy*, 700,

1–28.
https://doi.org/10.5852/ejt.2020.700

Mamonekene, V., Zamba, A.I. & Stiassny, M.L.J. (2018) A new small barb (Cyprininae: Smiliogastrini) from the Louesse, Lekoumou (upper Niari basin), and Djoulou (upper Ogowe basin) rivers in the Republic of Congo, west-central Africa. *American Museum Novitates*, 3917, 1–16.
https://doi.org/10.1206/3917.1

Mina, M.V., Golubtsov, A.S., Terefa, F., Tesfaye, G. & Dgebuadze, Yu.Yu. (2017) Studies of large and small barbs (genus *Barbus* sensu lato; Cyprinidae; Pisces) carried out by freshwater biology group of joint Ethio-Russian Biological Expedition (JERBE). *Ethiopian Journal of Biological Sciences*, 16 (Supplement), 21–44.

Nguyen, L.-T., Schmidt, H.A., von Haeseler, A. & Minh, B.Q. (2015) IQTREE: a fast and effective stochastic algorithm for estimating maximum-likelihood phylogenies. *Molecular Biology and Evolution*, 32 (1), 268–274.
https://doi.org/10.1093/molbev/msu300

Nutz, A., Schuster, M., Barboni, D., Gassier, G., Van Bocxlaer, B., Robin, C., Ragon, T., Ghienne, J.-F. & Rubino, J.-L. (2020) Plio-Pleistocene sedimentation in West Turkana (Turkana Depression, Kenya, East African Rift System): Paleolake fluctuations, paleolandscapes and controlling factors. *Earth-Science Reviews*, 211, 103415.
https://doi.org/10.1016/j.earscirev.2020.103415

Peters, W.C.H. (1852) Diagnosen von neuen Flussfischen aus Mossambique. *Bericht über die zur Bekanntmachung geeigneten Verhandlungen der Königlichen Preussischen Akademie der Wissenschaften zu Berlin*, 1852, 275–276 + 681–685. [in German]

Peters, W.C.H. (1868) Ueber eine von dem Baron Carl von der Decken entdeckte neue Gattung von Welsen, *Chiloglanis deckenii*, und einige andere Süsswasserfische aus Ostafrika. *Monatsberichte der Königlichen Preussischen Akademie der Wissenschaften zu Berlin*, 1868, 598–602. [in German]

Pfeffer, G.J. (1889) Übersicht der von Herrn Dr. Franz Stuhlmann in Ägypten, auf Sansibar und dem gegenüberliegenden Festlande gesammelten Reptilien, Amphibien, Fische, Mollusken und Krebse. *Jahrbuch der Hamburgischen Wissenschaftlichen Anstalten*, 6 (Art. 4), 1–36. [in German]

Pfeffer, G.J. (1896) *Die Thierwelt Ost-Afrikas und der Nachbargebiete*. Lieferung V. Die Fische Ost-Afrikas, 3, i–xviii + 1–72. [in German]

Prokofiev, A.M., Levin, B.A. & Golubtsov, A.S. (2021) A new species of *Enteromius* from the Bale Mountain Region, southeastern Ethiopia (Teleostei: Cyprinidae). *Ichthyological Exploration of Freshwaters*, 1161, 1–19.

Rambaut, A. (2018) FigTree. Version 1.4.4. Available from: https://github.com/rambaut/figtree/releases (accessed 30 March 2019)

Rambaut, A., Drummond, A.J., Xie, D., Baele, G. & Suchard, M.A. (2018) Posterior summarisation in Bayesian phylogenetics using Tracer 1.7. *Systematic Biology*, 67 (5), 901–904.
https://doi.org/10.1093/sysbio/syy032

Roberts, T.R. (1975) Geographical distribution of African freshwater fishes. *Zoological Journal of the Linnean Society*, 57 (4), 249–319.
https://doi.org/10.1111/j.1096-3642.1975.tb01893.x

Ronquist, F., Teslenko, M., van der Mark, P., Ayres, D.L., Darling, A., Hohna, S., Larget, B., Liu, L., Suchard, M.A. & Huelsenbeck, J.P. (2012) MrBayes 3.2: Efficient Bayesian Phylogenetic Inference and Model Choice across a Large Model Space. *Systematic Biology*, 61 (3), 539–542.
https://doi.org/10.1093/sysbio/sys029

Schmidt, R.C., Bart, Jr. H.L. & Nyingi, W.D. (2017) Multi-locus phylogeny reveals instances of mitochondrial introgression and unrecognized diversity in Kenyan barbs (Cyprininae: Smiliogastrini). *Molecular Phylogenetics and Evolution*, 111, 35–43.
https://doi.org/10.1016/j.ympev.2017.03.015

Schmidt, R.C., Bart, Jr. H.L. & Nyingi, W.D. (2018) Integrative taxonomy of the red-finned barb, *Enteromius apleurogramma* (Cyprininae: Smiliogastrini) from Kenya, supports recognition of E. amboseli as a valid species. *Zootaxa*, 4482 (3), 566–578.
https://doi.org/10.11646/zootaxa.4482.3.8

Seegers, L., De Vos, L. & Okeyo, D.O. (2003) Annotated checklist of the freshwater fishes of Kenya. *Journal of East African Natural History*, 92, 11–47.
https://doi.org/10.2982/0012-8317(2003)92[11:ACOTFF]2.0.CO;2

Skelton, P.H. (1980) *Systematics and Biogeography of the Redfin Barbus Species (Pisces: Cyprinidae) from Southern Africa.* PhD thesis, Rhodes University, Grahamstown, ix + 416 pp.

Skelton, P.H. (2001) *A Complete Guide to the Freshwater Fishes of Southern Africa*. Struik Publishers, Cape Town, 395 pp.

Tamura, K., Stecher, G. & Kumar, S. (2021) MEGA11: Molecular Evolutionary Genetics Analysis Version 11. *Molecular Biology and Evolution*, 38 (7), 3022–3027.
https://doi.org/10.1093/molbev/msab120

Van Ginneken, M., Decru, E., Verheyen, E. & Snoeks, J. (2017) Morphometry and DNA barcoding reveal cryptic diversity in the genus *Enteromius* (Cypriniformes: Cyprinidae) from the Congo basin, Africa. *European Journal of Taxonomy*, 310, 1–32.
https://doi.org/10.5852/ejt.2017.310

Whitehead, P.J.P. (1960) Three new cyprinid fishes of the genus *Barbus* from the Lake Victoria Basin. *Revue de Zoologie et de Botanique Africaines*, 62 (No. 1–2), 106–119.

Zhang, D., Gao, F., Jakovlić, I., Zou, H., Zhang, J., Li, W.X. & Wang, G.T. (2020) PhyloSuite: An integrated and scalable desktop platform for streamlined molecular sequence data management and evolutionary phylogenetics studies. *Molecular Ecology Resources*, 20, 348–355.
https://doi.org/10.1111/1755-0998.13096